An improved side-slip estimation algorithm based on ultra-local model technique for autonomous vehicles

Dániel Fényes, Tamás Hegedűs, Balázs Németh, Vu Van Tan, Péter Gáspár

***Abstract*— The paper presents a novel observer design method for estimating the front and rear wheel slips of the vehicle. The proposed observer design technique consists of two parts: A simple linear observer algorithm, which uses a reformulated lateral vehicle model to estimate the tire slips. The second part is based on an ultra-local model. The main goal of the ultra-local model is to eliminate the nonlinear, unmodeled, uncertain dynamics of the lateral vehicle model. In this way, the performance level of the linear observer can be significantly increased especially under critical circumstances such as high lateral acceleration maneuvers or driving on a low μ surface. The proposed observer algorithm is implemented in MATLAB/Simulink environment connected to the high-fidelity simulation software, CarMaker. The operation and the effectiveness of the proposed observer are demonstrated through several simulation examples.**

I. Introduction and motivation

The crucial prerequisite for the widespread of autonomous vehicles is the ability to operate in all possible traffic situations safely. Researchers and engineers often encounter roadblocks during their development of various functions. The algorithm, which is responsible for vehicle control, can be divided into layers such as sensing and observation, decision-making, and control layer. The accuracy of the states of the vehicles highly influences the performance level. Moreover, the stability requirements can also be insured through specific vehicle states, which are generally hardly measurable. This problem directs the attention of the developers towards solutions that can be used to estimate signals that are difficult or impossible to measure. Although, in the literature, several methods exist for the estimation problem, these approaches have their advantages and disadvantages.

In recent years, the attention from the classical, only model-based approaches started to shift towards data-driven methods. These solutions have drawbacks compared to the classical approaches: theoretical guarantee of stability, the quality and quantity of the dataset have a high influence on the performance level, and the accuracy in the unobserved operational range is low. Therefore, a new direction began to emerge, which tried to overcome the limitations of the methods by the combination of them.

Among the data-aided methods, a relatively new solution called the ultra-local model-based approach [1], can be mentioned. The main idea behind this approach is to approximate the nonlinearities and neglected dynamics of the system creating an ultra-local model, which is valid for a short time interval. This means, that the ultra-local model is recomputed at every sample time and, in the original concept, it is added to the control input. The advantage of this method is that no previously saved dataset is needed, and only uses measured and computed signals in online operation. Although the original method was created for control design, it has the potential to be used in estimation methods.

From the viewpoint of vehicle stability and control the accurate estimation of the lateral velocity, or the side slip angle is crucial. However, the main difficulty of the task comes from the fact, that the parameters of the vehicle change during its lifespan. Additionally, several external effects can influence the state of the vehicle, which leads to modeling difficulties. Since most of the classical estimation approaches mainly rely on an accurate model of the vehicle, the external effects and the unmodeled or neglected dynamics can significantly decrease the accuracy of the estimation process. On the other hand, efforts aimed at achieving a precise model of the vehicle result in a complex model, which leads to a challenging estimator design. This motivates the development of alternative solutions, in which methods with different operating principles are used parallelly.

Despite the classical approaches, such as the polytopic system-based approaches [2], Kalman filter-based [3], or the robust $\mathcal{H}_\infty$-based solutions [4], the data-aided approaches are also successfully applied for the lateral vehicle state estimation [5]. In paper, [6], a precise estimation approach is introduced for tire slip estimations using intelligent tire technology and machine-learning methodologies. During the measurements, additional sensors are deployed inside the tires, which measure the accelerations. The training process is achieved through frequency-domain features of accelerations which results in accurate estimation of the slip angles. Moreover, the driving force control can be enhanced through the estimation of the tire slip angle [7]. Paper [8] presents a tire slip angle estimation method, using piezoelectric film sensors (PVDF sensor), with which measurements can be performed. Then, three different machine learning approaches were trained for estimation purposes, and the

D. Fényes, T. Hegedűs, B. Németh and P. Gáspár are with HUN-REN Institute for Computer Science and Control (SZTAKI), Kende u. 13-17, H-1111 Budapest, Hungary. E-mail: [tamas.hegedus;daniel.fenyes]@sztaki.hu, [balazs.nemeth;peter.gaspar]@sztaki.hu

Vu Van Tan is with Department of Automotive Mechanical Engineering, Faculty of Mechanical Engineering, University of Transport and Communications, 3 Cau Giay Street, 100000 Hanoi, Vietnam E-mail: [vvtan@utc.edu.vn

The paper was funded by the National Research, Development and Innovation Office under OTKA Grant Agreement No. K 143599. The research was also supported by the National Research,Development and Innovation Office throughthe project "Cooperative emergency trajectory designfor connected autonomous vehicles" (NKFIH: 2019-2.1.12-TÉT VN). The work of Daniel Fényes was supported by the János Bolyai Research Scholarship of the Hungarian Academy of Sciences.

results showed that Gaussian process regression provided the most accurate results. Moreover, machine learning-based solutions are also suitable for tire slip estimation in off-road and unpaved surfaces [9].

In this paper, a combination of the ultra-local model-based and a classical approach can be found for tire side slip estimation. The classical approach is commonly used linear observer. The main advantage of the proposed method is that no previously saved, high amount of dataset is needed. Moreover, using the ultra-local model, the adaption of the varying parameters is also carried out. On the other hand, the simple design process of the estimation algorithm is also in the main focus. The presented solution does not require an accurate model of the vehicle. During the design of the linear observer, only the widely used two-wheeled bicycle model is used. Since the states of the bicycle model do not involve the tire slips, in the first step, it is modified to achieve the estimation process of these signals.

The rest of the paper consists of the following section. Firstly, the lateral model is presented, which is a reformulated version of the classical two-wheeled bicycle model, see Section II. In Section III, a brief introduction can be found to the applied methods namely: linear observer design and the ultra-local model. The design steps of the vehicle-oriented observer are also detailed in this section. The operation and the effectiveness of the proposed observer are demonstrated in Section IV. Finally, the contribution of the paper is summarized in Section V.

II. Modeling of lateral dynamics

The lateral dynamics of the vehicle is modeled by the modified version of the single-track bicycle model. The original bicycle model consists of the main equations: lateral, and the yaw-motion, see [10]:

$$I_z\ddot{\psi} = \mathcal{F}_f(\alpha_f)l_f - \mathcal{F}_r(\alpha_r)l_r, \tag{1a}$$

$$mv_x(\dot{\psi}+\dot{\beta}) = \mathcal{F}_f(\alpha_f) + \mathcal{F}_r(\alpha_r), \tag{1b}$$

where the parameters are: l_f, l_r are the distances of the rear/front axles from the center of gravity (CoG), $\mathcal{F}_f, \mathcal{F}_r$ are the lateral forces, α_f, α_r are the tire slips, I_z represents the yaw inertia, m is the mass of the vehicle, v_x is the longitudinal velocity, $\dot{\psi}$ is the yaw-rate and $\beta = atan\frac{v_y}{v_x}$ is the side-slip of the vehicle. Slips can be expressed in a linear form as: $\alpha_f = \delta - \beta - \frac{\dot{\psi}l_f}{v_x}$, $\alpha_r = -\beta + \frac{\dot{\psi}l_r}{v_x}$ functions of the steering angle (δ), β, $\dot{\psi}$ and v_x.

A. Model with slips as states

The states of the original bicycle model can be changed to the slips by reordering the equations (1), see [11]:

$$\dot{\psi} = v_x\frac{\alpha_r - \alpha_f + \delta}{l_f + l_r}, \tag{2a}$$

$$\beta = -\frac{\alpha_f l_r + \alpha_r l_f - l_r\delta}{l_f + l_r}. \tag{2b}$$

In the next step, the derivatives of yaw-rate and side-slip are derived as:

$$\ddot{\psi} = v_x\frac{\dot{\alpha}_r - \dot{\alpha}_f + \dot{\delta}}{l_f + l_r}, \tag{3a}$$

$$\dot{\beta} = -\frac{\dot{\alpha}_f l_r + \dot{\alpha}_r l_f - l_r\dot{\delta}}{l_f + l_r}. \tag{3b}$$

The derivative of the longitudinal velocity is not computed since it is assumed to be constant for the given time interval. Subtracting (1) from (3), the derivative of the tire slips can be computed:

$$\dot{\alpha}_r - \dot{\alpha}_f = \frac{l_f + l_r}{I_z}\big(\mathcal{F}_f(\alpha_f)l_f - \mathcal{F}_r(\alpha_r)l_r\big) - \dot{\delta}, \tag{4a}$$

$$\dot{\alpha}_f l_r + \dot{\alpha}_r l_f = v_x(\alpha_r - \alpha_f) + v_x\delta + l_r\dot{\delta} - \frac{l_f + l_r}{mv_x}\big(\mathcal{F}_f(\alpha_f) + \mathcal{F}_r(\alpha_r)\big). \tag{4b}$$

Note that the derivative of the steering angle ($\dot{\delta}$) appears in the equations above. It is approximated with an upper bound as $\dot{\delta} \approxeq max\Big(\frac{|\dot{\delta}|}{|\delta|}\Big)\delta = \varphi\delta$.

B. State-space representation of the modified model

The reformulated model can be transformed into a state-space representation using the cornering stiffness (C_i) instead of the lateral force: $\mathcal{F}_i = C_i\alpha_i$, $i = \{f, r\}$, where f indicates the front, while r is the the rear axle. Furthermore, the state-space is extended with an additional state, the yaw-rate using (1)(a) to improve the performance of the observer, which will be detailed in Subsection III-C.

$$\dot{x}_v = A_v x_v + B_v u_v, \tag{5a}$$

$$y_v = C_v^T x_v, \tag{5b}$$

$$\underbrace{\begin{bmatrix}\dot{\alpha}_f\\ \dot{\alpha}_r\\ \ddot{\psi}\end{bmatrix}}_{\dot{x}_v} = \underbrace{\begin{bmatrix}a_{11} & a_{12} & 0\\ a_{21} & a_{22} & 0\\ a_{31} & a_{32} & 0\end{bmatrix}}_{A_v(\rho)}\begin{bmatrix}\alpha_f\\ \alpha_r\\ \dot{\psi}\end{bmatrix} + \underbrace{\begin{bmatrix}b_1\\ b_2\\ 0\end{bmatrix}}_{B_v}\delta, \tag{5c}$$

$$\underbrace{\begin{bmatrix}ma_y\\ \dot{\psi}\end{bmatrix}}_{y_v} = \underbrace{\begin{bmatrix}C_f & C_r & 0\\ 0 & 0 & 1\end{bmatrix}}_{C^T}\begin{bmatrix}\alpha_f\\ \alpha_r\\ \dot{\psi}\end{bmatrix}. \tag{5d}$$

where $ma_y = mv_x(\dot{\beta} + \dot{\psi})$.
Other parameters of the state-matrices are:

$$a_{11} = -\frac{C_f l_f^2}{I_z v_x} - \frac{v_x}{l_f + l_r} - \frac{C_f}{mv_x(t)}, \tag{6a}$$

$$a_{12} = \frac{C_r l_f l_r}{I_z v_x} + \frac{v_x}{l_f + l_r} - \frac{C_r(t)}{mv_x}, \tag{6b}$$

$$a_{21} = \frac{C_f l_r l_f}{I_z v_x} - \frac{v_x}{l_f + l_r} - \frac{C_f}{mv_x}, \tag{6c}$$

$$a_{22} = -\frac{C_r l_r^2}{I_z v_x} + \frac{v_x}{l_f + l_r} - \frac{C_r}{m v_x}, \tag{6d}$$

$$a_{31} = \frac{C_f l_f}{I_z}, \quad a_{32} = -\frac{C_r l_r}{I_z}, \tag{6e}$$

$$b_1 = \frac{v_x}{l_f + l_r} + \varphi, \quad b_2 = \frac{v_x}{l_f + l_r}. \tag{6f}$$

III. Applied methods for observer design

In this section, the applied methods for the observer design are presented. Firstly, the main concepts of the Model-Free Control and the ultra-local model are detailed. Then, the linear observer design process is briefly described.

A. Ultra-Local Model and Model-Free Control

The Model-Free Control and the ultra-local model-based control technique was presented by M. Fliess at al in [12]. This method can cope with the uncertain, nonlinear dynamics of the considered system by applying a so-called ultra-local model:

$$y_{ulm}^{(\nu)} = F + \alpha u, \tag{7}$$

where F is the ultra-local model, ν derivative order, y_{ulm} is the measured output, α is a tuning parameter of this model and the control input is denoted by u.
Using the previous equation, the ultra-local model is computed as:

$$F = y_{ulm}^{(\nu)} - \alpha u \tag{8}$$

The main goal of the ultra-local model is to eliminate the derivative of the error signal:

$$e^{(\nu)} = y_{ulm}^{(\nu)} - y_{ref}^{(\nu)} = F + \alpha u - y_{ref}^{(\nu)} \tag{9}$$

where y_{ref} is the reference signal. This can be achieved by using u as the control signal:

$$u = \frac{-F + y_{ref}^{(\nu)}}{\alpha} \tag{10}$$

In a control-oriented application, the tracking performance is also a crucial factor, therefore an additional controller is applied denoted by $K(s)$ However, it cannot guarantee the zero steady-state error in terms of the error signal ($e = y_{ref} - y$) thus an additional controller ($K(s)$) is applied:

$$u_{\text{ulm}} = \frac{-F + y_{ref}^{(\nu)} + K(s)e}{\alpha} \tag{11}$$

the technique behind $K(s)$ can be freely chosen, see [12], [13]. So, in the general case, the MFC strategy has two controller signals: one from the ultra-local model, which aims to eliminate the unknown dynamics of the system, and the additional controller, whose role is to guarantee the tracking performance.
In the case of observer design, only the ultra-local model is used since there is no need for tracking performance.

B. Linear Observer

Linear observer design is based on the state-space representation of the considered system. A general state-space representation is given in discrete form as:

$$x(t+1) = \phi x(t) + \Gamma u(t), \tag{12a}$$

$$y(t) = C^T x(t), \tag{12b}$$

where ϕ, Γ, C are matrices, $x(t)$ consists of the states of the system, $u(t)$ denotes the control input whilst $y(t)$ is output vector The main goal is to eliminate the error between the measured states ($x(t)$) and the estimated ones ($\hat{x}(t)$)

$$e(t) = x(t) - \hat{x}(t), \qquad |e| \to min! \tag{13}$$

The state equation of the observer, see [14]:

$$\hat{x}(t+1) = \phi \hat{x}(t) + \Gamma u(t) + L_d(C\hat{x}(t) - y(t)). \tag{14}$$

L_d is the observer gain vector. The gains can be computed by minimizing the following cost function:

$$J = \frac{1}{2} \sum_{i=1}^{\infty} (x^T(t) Q x(t) + u^T(t) R u(t)) \tag{15}$$

where Q and R are weighting matrices. The optimal gain vector can be obtained by solving the Ricatti equation for P:

$$\phi^T P \phi - P + Q - \phi^T P \Gamma (R + \Gamma^T P \Gamma)^{-1} \Gamma^T P \phi = 0 \tag{16}$$

Using P the optimal gain vector can be determined as:

$$L_d = -(R + \Gamma^T P \Gamma)^{-1} \Gamma^T P \phi \tag{17}$$

C. Observer design

In this section, the combined observer design is presented using detailed methods, namely the ultra-local model and the linear observer. The main steps of the design process are the following:

1) As a first step, a nominal model is needed. In this case, the modified bicycle model is used presented in Section II. The continuous model must be discretized for the implementation, see [15]. In this case, the model is discretized with $T_s = 0.01s$ and using ZOH technique. The computed discrete model is denoted by $x_v(t) = \phi_v x(t) + \Gamma_v u(t), y_v(t) = C^T x(t)$
   The measured outputs (y_v) are the lateral acceleration (a_y) and the yaw-rate ($\dot{\psi}$), see (5c).
2) Design of the linear observer as detailed in Section III.
3) The ultra-local model needs an output (y) and the order of derivative (ν). The selected output is $y_{ulm} = a_y$ and derivative order is selected to $\nu = 1$, which means $\dot{y}_{ulm} = \dot{a}_y$.
4) Selection of derivative algorithm, ALIEN filter is a frequently used technique for computing a derivative of a noisy, measured signal, therefore it is suitable for this application. ALIEN filter algorithm is detailed in [16].
5) Next step is the tuning of the free parameter α. There are several iterative algorithms to get the optimal value for α. In this study, the authors' previous method is used, which is detailed in [17].

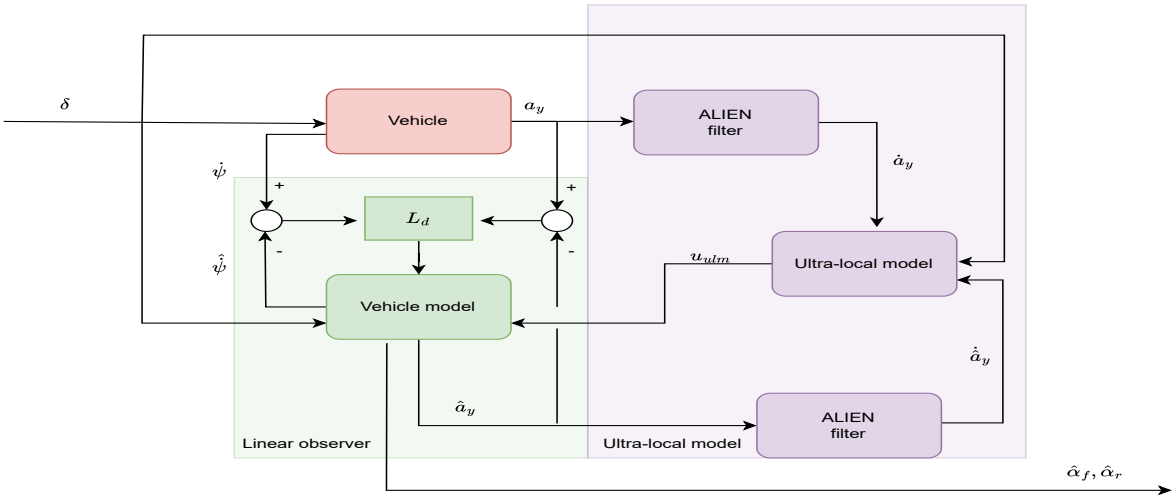

Fig. 1. Schematic structure of the observer

6) Interconnection of the whole algorithm. The state equation of the interconnected observer is in the discrete form: $\hat{x}(t+1) = \phi_v \hat{x}(t) + \Gamma_v[u(t) + u_{ulm}(t)] + L_d(\hat{y}(t) - y(t))$
where ϕ_v and Γ_v are the discrete state matrices, while L_d is the discrete observer gain vector.

The structure of the whole algorithm is illustrated in Figure 1. During the estimation of the tire slips only cost-efficiently and accurately measurable signals are used: the lateral acceleration and the yaw-rate. Based on these signals, the unmodeled dynamics, which are neglected during the linear observer design are considered. Moreover, the external influences can be handled by the ultra-local model-based part. Since the ultra-local model is capable of handling the parameter uncertainty of the system, the complexity of the classical observer design is significantly decreased.

IV. Simulation

In this section, simulation examples are presented to show the operation and the effectiveness of the proposed observer algorithm. The whole algorithm is implemented in MATLAB/Simulink environment, which is connected to the high-fidelity simulation software, CarMaker. The selected vehicle is an electric car, namely the Tesla Model S. The main parameters of the vehicle can be found in Table IV. During the tests, the vehicle is driven by the CarMaker inbuilt driver on a track shown in Figure 2. The simulation examples include three different test scenarios: a test with high longitudinal velocity, a test with varying longitudinal velocity, and a test with low adhesion coefficient. The results of the combined method are also compared to a standard linear observer.

A. High lateral acceleration

In the first scenario, the vehicle is driven along the test track at a high longitudinal velocity as shown in Figure 3. The parameters of the linear observer are the same as in Table IV and the longitudinal velocity is set to $v_x = 22m/s$. The estimated and the real slips are shown in Figure 5. As it can be seen, both observers can estimate the front slip with a high accuracy except for some peaks where the linear observer has a significant error around $\approx 25\%$. At that peak, the vehicle dynamics are in the nonlinear region, which cannot be handled by a linear observer. However, the combined algorithm can deal with these unmodeled dynamics by providing an additional control signal as shown in Figure 4. Finally, the yaw-rate is illustrated in Figure 6. The maximal value of the yaw-rate is around $\dot{\psi} = 0.55rad/s$, which is close to the physical limits of a standard passenger vehicle.

m	2100 (kg)
l_f, lr	1.5, 1.5 (m)
I_z	3900 (kgm^2)
ϕ	0.4 $\frac{1}{s}$

TABLE I
Parameters of the test vehicle

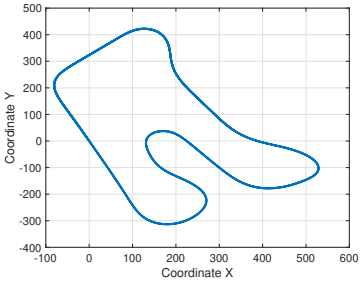

Fig. 2. Track

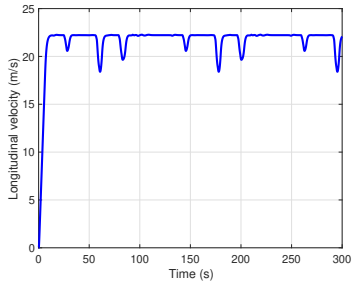

Fig. 3. Longitudinal velocity

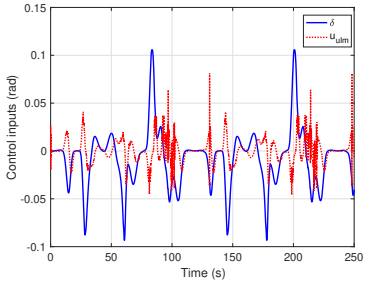

Fig. 4. Control inputs

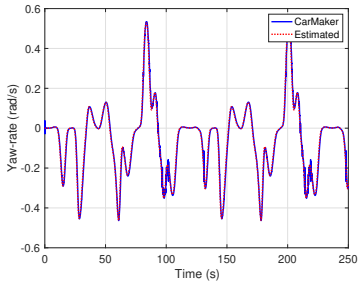

Fig. 6. Yaw-rate

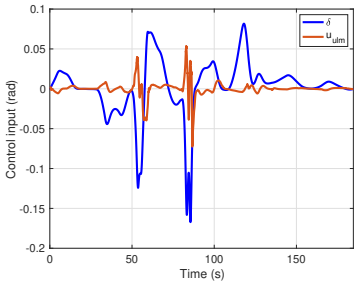

Fig. 7. Control inputs

B. Test with varying longitudinal velocity

In the next test scenario, both observers are tested on the same track with varying longitudinal velocities. The longitudinal velocity profile is illustrated in Figure 9. The speed varies between $10m/s$ and $20m/s$. Since the nominal vehicle model highly relies on the longitudinal velocity, using the linear observer, this radical change cannot be handled properly. Therefore, only the results of the combined solution is presented. The real and the estimated slips are depicted in Figure 8. The proposed combined observer is able to estimate the slip in the whole range of the longitudinal velocity. The control inputs are in Figure 7. The maximal value of the output of the ultra-local model is around $t = 55s$ and $t = 90s$, where the slip reaches its peak values and the nonlinearities of the vehicle are the most significant. Finally, the yaw-rate of this case is illustrated in Figure 10.

C. Test on low μ surface

In the last case, the vehicle is driven on a surface with a low adhesion coefficient $\mu = 0.5$ to show that the proposed observer can deal with this drastic change. The velocity profile is similar to the first case, set to $v_x = 22m/s$ and it is reduced at sharp bends to avoid the unstable motion of the vehicle. The measured and the estimated slips are depicted in Figure 12. The estimation has a lower accuracy compared to the previous cases but the average error remains under $< 3\%$, which is still an acceptable value. Finally, the yaw-rate is shown in Figure 13. The maximal value is declined to $\dot{\psi} = 0.4rad/s$, which is caused by the low adhesion coefficient.

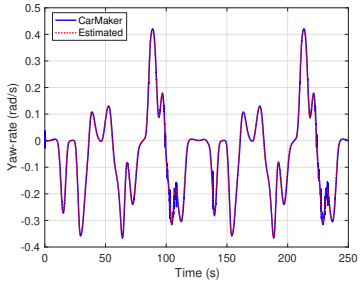

Fig. 13. Yaw-rate

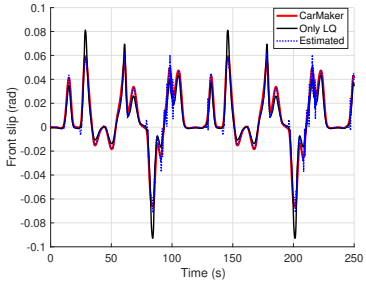

Fig. 5. Slip angles

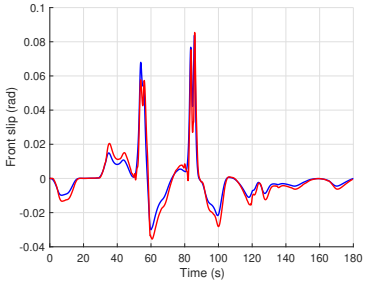

Fig. 8. Slips angles

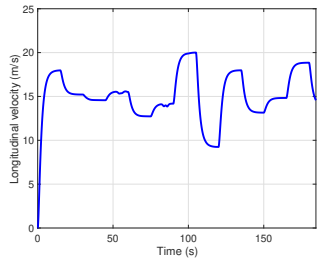

Fig. 9. Longitudinal velocity profile

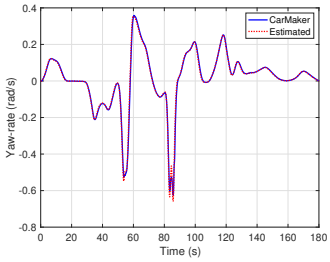

Fig. 10. Yaw-rate

V. Conclusion and Future Work

The paper proposed a novel observer design method to estimate the side slips of the vehicle. The presented strategy had two main parts: a classical linear observer and an ultra-local model. The combined observer could deal with the unmodeled, nonlinear, uncertain dynamics of the vehicle, thus providing a high-performance level even under extreme circumstances. The proposed observer has been implemented and tested in MATLAB/Simulink environment with connection to the high-fidelity simulation software, CarMaker. The detailed simulation has shown the algorithm could estimate the slips with a high accuracy.

References

[1] M. Fliess and C. Join, "Model-free control," *International Journal of Control*, vol. 86, no. 12, pp. 2228–2252, Dec 2013.

[2] A.-J. Perez-Estrada, G.-L. Osorio-Gordillo, M. Darouach, M. Alma, and V.-H. Olivares-Peregrino, "Generalized dynamic observers for quasi-lpv systems with unmeasurable scheduling functions," *International Journal of Robust and Nonlinear Control*, vol. 28, no. 17, pp. 5262–5278, 2018.

[3] S. Sen, S. Chakraborty, and A. Sutradhar, "Estimation of tire slip-angles for vehicle stability control using kalman filtering approach," in *2015 International Conference on Energy, Power and Environment: Towards Sustainable Growth (ICEPE)*, 2015, pp. 1–6.

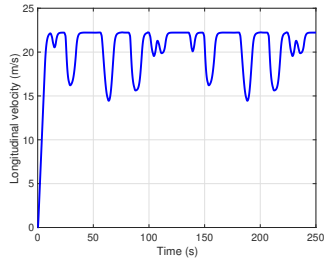

Fig. 11. Longitudinal velocity profile

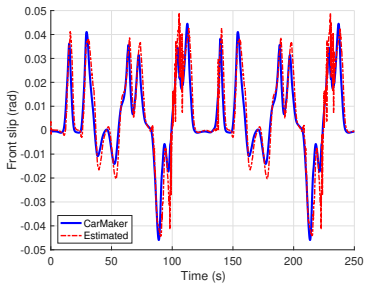

Fig. 12. Slip angles

[4] J. Jung, K. Huh, H. Fathy, and J. Stein, "Optimal robust adaptive observer design for a class of nonlinear systems via an h-infinity approach," pp. 6 pp.–, 2006.

[5] Y. Wang and S. Deprizon, "A data-driven estimation algorithm for vehicle side-slip angle," in *2023 International Symposium on Intelligent Robotics and Systems (ISoIRS)*, 2023, pp. 18–21.

[6] N. Xu, Y. Huang, H. Askari, and Z. Tang, "Tire slip angle estimation based on the intelligent tire technology," *IEEE Transactions on Vehicular Technology*, vol. 70, no. 3, pp. 2239–2249, 2021.

[7] H. Fuse and H. Fujimoto, "Fundamental study on driving force control method for independent-four-wheel-drive electric vehicle considering tire slip angle," in *IECON 2018 - 44th Annual Conference of the IEEE Industrial Electronics Society*, 2018, pp. 2062–2067.

[8] X. Sun, Z. Quan, Y. Cai, L. Chen, and B. Li, "Intelligent tire slip angle estimation based on sensor targeting configuration," *IEEE Transactions on Instrumentation and Measurement*, vol. 73, pp. 1–16, 2024.

[9] M. Basri, A. Karapetyan, B. Hassan, M. Khonji, and J. Dias, "A hybrid deep learning approach for vehicle wheel slip prediction in off-road environments," in *2022 IEEE International Symposium on Robotic and Sensors Environments (ROSE)*, 2022, pp. 1–7.

[10] J. Hahn, R. Rajamani, S. You, and K. Lee, "Real-time identification of road-bank angle using differential GPS," *IEEE Transactions on Control Systems Technology*, vol. 12, pp. 589–599, 2004.

[11] T. P. Balazs Nemeth, Peter Gaspar, "Nonlinear analysis of vehicle control actuations based on controlled invariant sets," *International Journal of Applied Mathematics and Computer Science*, vol. 26, no. 1, pp. 31–43, 2016. [Online]. Available: http://eudml.org/doc/276550

[12] M. Fliess and C. Join, "Model-free control and intelligent PID controllers: Towards a possible trivialization of nonlinear control?" *Proc. 15th IFAC Symposium on System Identification, Saint-Malo, France*, vol. 42, pp. 1531–1550, 2009.

[13] Y. A. Younes, A. Drak, H. Noura, A. Rabhi, and A. El Hajjaji, "Robust Model-Free Control Applied to a Quadrotor UAV," *Journal of Intelligent and Robotic Systems*, vol. 84, pp. 37 – 52, Dec. 2016.

[14] C. M. Kang and W. Kim, "Linear parameter varying observer for lane estimation using cylinder domain in vehicles," *IEEE Transactions on Intelligent Transportation Systems*, pp. 1–10, 2020.

[15] R. Tóth, *Discretization of LPV Systems*. Berlin, Heidelberg: Springer Berlin Heidelberg, 2010, pp. 143–169.

[16] P. Polack, S. Delprat, and B. dAndrea Novel, "Brake and velocity model-free control on an actual vehicle," *Control Engineering Practice*, vol. 92, pp. 1–8, 2019.

[17] T. Hegedus, D. Fenyes, B. Nemeth, Z. Szabo, and P. Gaspar, "Design of model free control with tuning method on ultra-local model for lateral vehicle control purposes," in *2022 American Control Conference*, 2022.